Numerical studies of a low-loss and broad-pass-band single-sided-structure left-handed metamaterial

Jianhong Lv,* Baorong Yan, Minghai Liu, and Xiwei Hu†
College of Electrical and Electronic Engineering, Huazhong University of Science and Technology, Wuhan 430074, People's Republic of China
(Received 19 September 2008; published 15 January 2009)

A single-sided structure left-handed metamaterial (LHM), of which the symmetric paired split-ring resonators are connected directly through cut wires, is discussed in this paper. This connected single-sided LHM can exhibit a low loss and broad negative refraction passband. Good agreement of the retrieved result and the simulated result verify the above conclusion by comparison with the in-plane case and the off-plane case [T. Koschny, M. Kafesaki, E. N. Economou, and C. M. Soukoulis, Phys. Rev. Lett. **93**, 107402 (2004)].

DOI: 10.1103/PhysRevE.79.017601 PACS number(s): 41.20.Jb, 42.25.Bs, 78.20.Ci

I. INTRODUCTION

In the past several years, left-handed metamaterials (LHMs), which were first named and theoretically discussed by Veselago [1], have been extensively studied. They have simultaneously negative permittivity ($\varepsilon<0$) and negative permeability ($\mu<0$), and they can exhibit different physical properties from the materials in nature, such as negative refraction and reversal of the Doppler effects. The first LHM, which consisted of arrays of split-ring resonators (SRRs) and wires, was constructed and experimentally demonstrated by Smith *et al.* in 2000 [2] based on the spirit of Pendry *et al.* [3,4], where the array of SRRs and the array of wires can exhibit negative permeability and negative permittivity, respectively. Then many groups [5–11] constructed LHMs by printing the SRRs and the wires on both sides of the substrates. In the gigahertz range, there is no difficulty in fabricating these two sided LHMs, but at high frequencies, such as terahertz, it is difficult to print the metal wires on both sides of the substrate. So Bayindir and co-workers [12,13] proposed single-sided LHMs where the SRRs and the wires are both printed on one side of the substrates. However, these single-sided LHMs have higher loss and narrower passband than two-sided cases [14,15]. In order to avoid problems of high loss, narrow passband, and difficult fabrication, we propose a single-sided LHM, which consists of symmetric paired split-ring resonators (SPSRRs) [7,16,17] and cut wires connecting to each other in this paper. This single-sided LHM can exhibit a low loss and broad negative refraction passband.

II. NUMERICAL ANALYSIS

The unit cell of a symmetric paired split-ring resonator (SPSRR) with geometric scales is shown in Fig. 1(a), where the 0.03-mm-thick copper wires are printed on one side of the FR-4 substrate (relative dielectric constant $\varepsilon_r=4.6$), and other dimensions are displayed in the caption under Fig. 1. The array of SPSRRs combined with the continuous wires or cut wires can exhibit negative refraction in a certain frequency band. Here, we give three different combined configurations as shown in Figs. 1(b)–1(d); the difference between those configurations is the position of the wires with respect to the SPSRRs. The width of the continuous wires and the cut wires are all 0.4 mm. In those configurations, the off-plane configuration of Fig. 1(c) and the in-plane configuration of Fig. 1(d) have been discussed and compared in earlier works [14,15]. For the connected case (SRRs are connected directly through the cut wires) as shown in Fig. 1(b), a structured array of this configuration is shown in Fig. 1(e), where the unit cell of Fig. 1(b) is a periodic arrangement in the x, y, and z directions, respectively. By comparing with the in-plane configuration [Fig. 1(d)] and the off-plane configuration [Fig. 1(c)], we will discuss the low loss and broad passband of the connected single-sided structure LHM numerically.

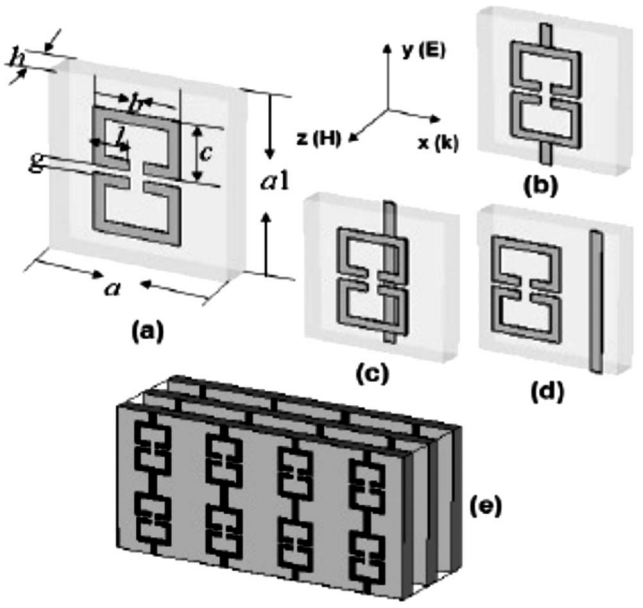

FIG. 1. (a) The unit cell of the symmetrical paired split-ring resonator with the geometric dimensions $a=a1=5$ mm, $b=2.4$ mm, $c=1.6$ mm, $l=1$ mm, $g=0.2$ mm, and $h=1$ mm. The metal wires of SPSRRs are 0.3 mm in width. Three configurations of (b) the connected case, (c) the off-plane case, (d) the in-plane case. (e) The array of the periodic arrangement of the connected case.

*lvjianhong@smail.hust.edu.cn
†xwhu@mail.hust.edu.cn

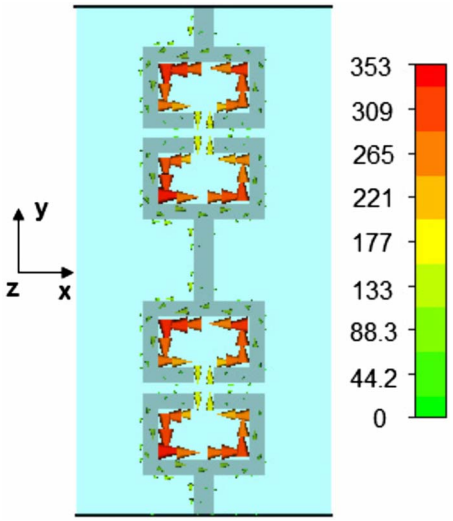

FIG. 2. (Color online) Distribution of the induced current in the copper wires at a frequency just above the resonance.

In the connected case, another different configuration has been studied by Liu *et al.* [18], where the subwavelength size resonators interact mainly through the exchange of a conducting current, resulting in stronger coupling as compared to the corresponding magnetoinductive interaction. Unlike that for the connected configuration as shown in Fig. 1(b), the magnetoinductive interaction is the dominant coupling mechanism as in the other two configurations as shown in Figs. 1(c) and 1(d). The distribution of the induced current in the copper wires is shown in Fig. 2. The strong magnetoinductive current, which circled the SPSRRs' loop, exhibits a self-inductance (L). This inductance combines with the capacitance (C) between the arms of the SPSRRs forming a LC resonant circuit, and then exhibits a negative magnetic response. The cut wires together with the SPSRRs exhibit a negative electric response. Here, the incident electromagnetic wave is polarized with the magnetic field perpendicular to the SPSRR plane ($\mathbf{H} \| z$) and the electric field parallel to the cut wires ($\mathbf{E} \| y$). Consequently, the propagation direction ($\mathbf{k}$) is along the x axis. In our numerical simulation, this polarized incidence condition is satisfied throughout this Brief Report by applying the corresponding perfect magnetic conductor (PMC), perfect electric conductor (PEC), and open boundaries (corresponding to the boundaries perpendicular to the z, y, and x axes, respectively).

For the connected configuration metamaterial, it is actually a bianisotropic medium for the coupling between its electric and magnetic response. But in retrieving the effective constitutive parameters of this homogeneous metamaterial, the weak bianisotropic effect can be neglected and the generally used retrieval procedure [19,20] is adopted. Here, we retrieve the effective constitutive parameters of three configurations to be compared. The reflection S_{11} and transmission S_{21} scattering data that the effective constitutive parameters are retrieved from are simulated by the software CST MICROWAVE STUDIO. The retrieved effective refraction index n, effective permeability μ, effective permittivity ε, and effective impedance Z of three configurations are plotted in Figs. 3(a)–3(d), where the solid line, the dotted line, and the dashed-dotted line denote the configurations of Figs. 1(b)–1(d), respectively. From Figs. 3(a)–3(d), we find that three configurations can all exhibit a negative refraction index in a certain frequency range. The negative refraction band of the connected configuration [Fig. 1(b)] (7.5–8.3 GHz) is nearly equal to the off-plane configuration [Fig. 1(c)] (7.5–8.2 GHz). But for the in-plane configuration [Fig. 1(d)], the negative refraction band (8.2–8.4 GHz) is much narrower than the other two configurations. Furthermore, from Fig. 3(d), we get that the impedance at the surface of the metamaterial slab of the in-plane configuration is mismatched, and therefore it will affect the transmission of this configuration.

In order to verify the low-loss transmission of the connected configuration [Fig. 1(b)], we plot the simulated transmissions of three configurations versus frequency as is shown in Fig. 4. Here, the simulated transmissions are also obtained by the software CST MICROWAVE STUDIO. In the simulation, the array of three configurations [Fig. 1(b)–1(d)] all have $N_x=10$, $N_y=2$, and $N_z=15$ unit cells, with periodic arrangement of $a_x=5$ mm, $a_y=5$ mm, and $a_z=3$ mm, respectively. From Fig. 4, we find that the connected configuration of Fig. 1(b) (the dotted line) exhibits a low-loss negative refraction passband as the off-plane configuration of Fig. 1(c) (the dashed-dotted line) with the peak about −2 dB, and for the in-plane configuration of Fig. 1(d) (the solid line), it exhibits a very high loss with the transmission peak only about −57 dB. The high loss of this single-sided in-plane configuration makes it not the best selection for application even though it is easily fabricated, but the single-sided connected configuration shown in Fig. 1(b) can easily avoid this problem. The widths of the negative refraction passband of three configurations agree well with the theoretical results as shown in Fig. 3.

For the off-plane configuration, Markos *et al.* [21] have pointed out that the size of the unit cell can affect the width of negative refraction passbands of LHMs. The transmission peaks for LHMs are broader for a smaller unit cell, but this is not always tenable, because the SRR not only can exhibit a magnetic response, but can also exhibit an electric response as the cut wires [14]. The coupling between the SRRs and the wires decreases the plasma frequency (ω_p) of the wires alone to a lower effective plasma frequency (ω_p') of the SRRs and wires. Sometimes, the effective plasma frequency (ω_p') may be lower than the magnetic plasma frequency (ω_{mp}) of the SRRs, and the negative refraction passband will be narrowed. But with the connected configuration, the effective plasma frequency is much less sensitive to the changing of the dimensions of the unit cell as compared to the off-plane configuration. So we can still get a broad negative refraction passband with a decrease in the geometric dimensions of the unit cell of this configuration. To verify these conclusions, we change the geometric dimensions of the unit cell for $a=4.3$ mm, $a1=3.3$ mm, $b=2.6$ mm, $c=1.2$ mm, $l=0.8$ mm, $g=0.2$ mm, and $h=1$ mm. The width of the wires and the cut wires is 0.3 mm. The simulated transmissions and the retrieved part of refraction indices versus frequency are plotted and compared in Figs. 5(a) and 5(b) where the solid line and the dotted line in Fig. 5 denote the connected configuration [Fig. 1(b)] and the off-plane configuration [Fig. 1(c)], respec-

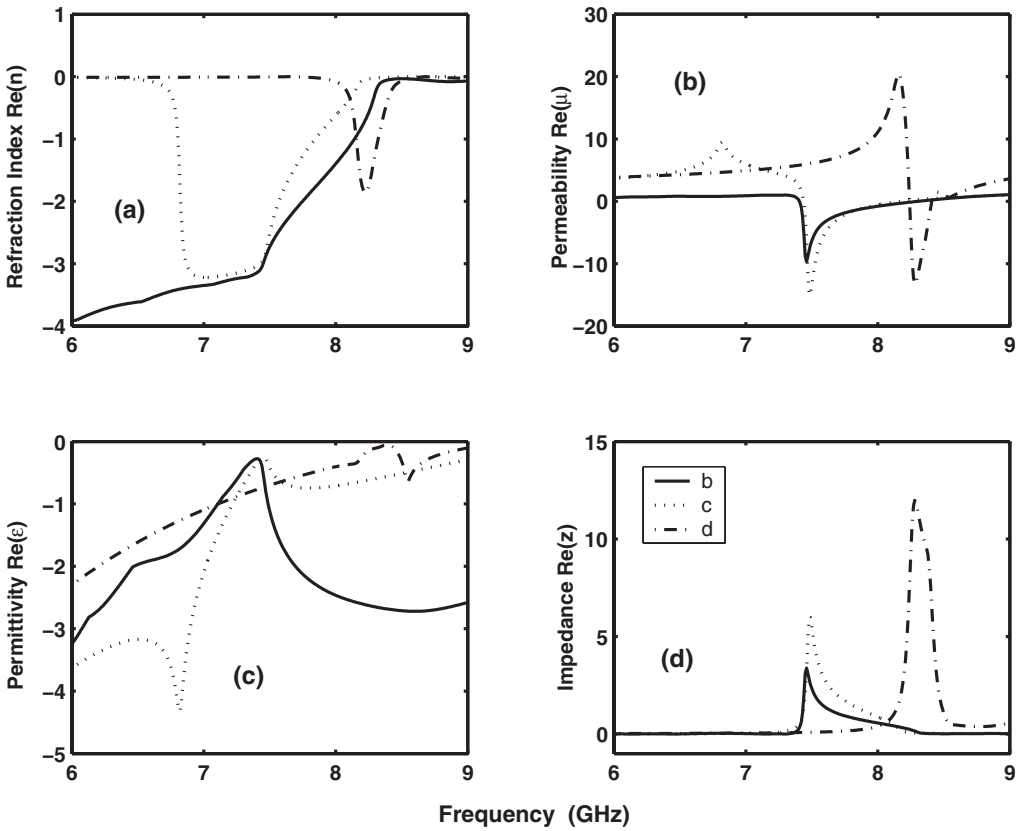

FIG. 3. The retrieved refraction index n (a), permeability (b), permittivity (c), and impedance (d); the solid line, the dotted line, and the dashed-dotted line denote the connected configuration [Fig. 1(b)], the off-plane configuration [Fig. 1(c)], and the in-plane configuration [Fig. 1(d)], respectively.

tively. From Figs. 5(a) and 5(b), we find that the simulated results and the retrieved results agree well; the negative refraction passband of the connected configuration (9–10.6 GHz) is broader than the off-plane configuration (9–10.2 GHz). The broadened passband of the connected configuration may be due to the stronger coupling among neighboring unit cells along the propagation direction (in the x direction) with a decrease in the constant ($a=5$ mm$\rightarrow a=4.3$ mm) in this direction. The effective plasma frequency

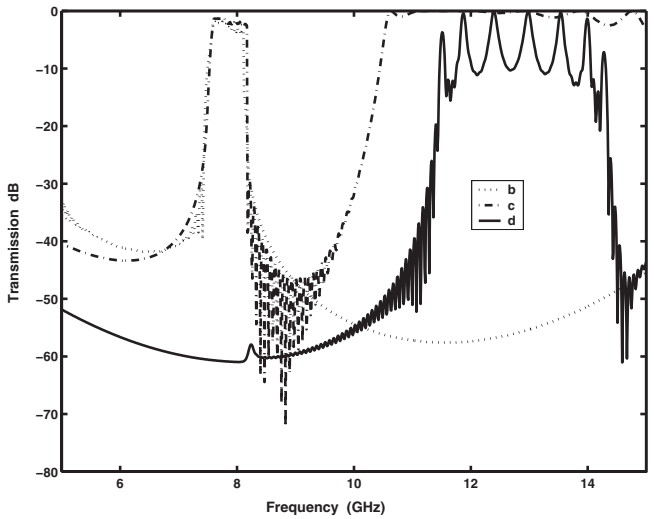

FIG. 4. Simulated transmissions of three configurations: the dotted line, the dashed-dotted line, and the solid line denote the connected configuration [Fig. 1(b)], the off-plane configuration [Fig. 1(c)], and the in-plane configuration [Fig. 1(d)], respectively.

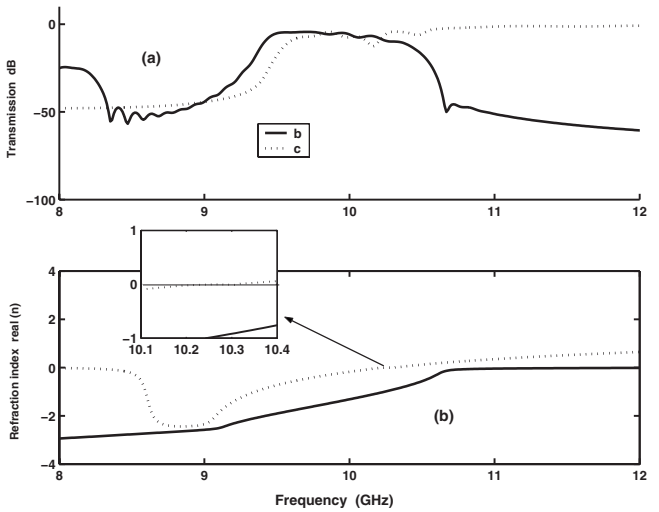

FIG. 5. Simulated transmissions (a) and the retrieved real part of the refraction index (b) versus the frequency of the connected configuration [Fig. 1(b)] and the off-plane configuration [Fig. 1(c)]. The solid line and the dotted line denote the connected and the off-plane configurations, respectively.

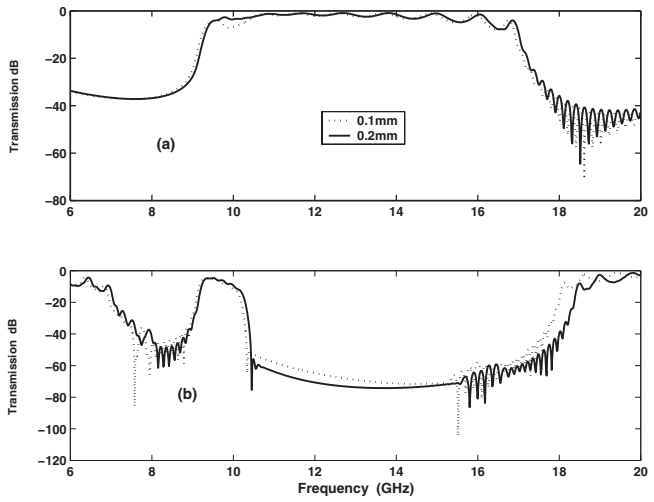

FIG. 6. Simulated transmissions of the off-plane configuration (a) and the connected configuration (b). The dotted line and the solid line denote that the widths of the wires or cut wires are 0.1 and 0.2 mm, respectively.

(ω_p') of the off-plane configuration is only about 0.1 GHz higher than the magnetic plasma frequency (ω_{mp}) as shown in the inset of Fig. 5(b). If we further decrease some geometric dimensions of the unit cell, such as the width of the wire, the effective plasma frequency (ω_p') of the off-plane configuration may be equal to or lower than its magnetic plasma frequency (ω_{mp}). Here, we decrease the widths of wires and cut wires from 0.3 mm to 0.1 and 0.2 mm, respectively, and plot the simulated transmissions of two configurations in Figs. 6(a) and 6(b). When the width of the wire decreases to 0.2 mm, there is no band gap between the left-handed passband and the right-handed passband [solid line in Fig. 6(a)], because the effective plasma frequency is equal to the magnetic plasma frequency $(\omega_p'=\omega_{mp})$. In this case, the structure is a balanced composite structure [22]. With 0.1-mm-wide wires, the effective plasma frequency is lower than the magnetic plasma frequency for the off-plane configuration [the dotted line in Fig. 6(a)], and the negative refraction passband is further narrowed. For the connected configuration, the simulated results are shown in Fig. 6(b), where the effective plasma frequency (ω_p') and the width of the negative refraction passband are nearly insensitive to the changing of the width of cut wires. So, when some geometric dimensions of the unit cell decrease to small sizes, we can still get a broad negative refraction passband with this single-sided-connected configuration LHM as compared to the off-plane configuration.

III. CONCLUSION

In conclusion, we have proposed a single-sided structure metamaterial, which consists of symmetric paired split-ring resonators (SPSRRs) and the cut wires, to exhibit the left-handed properties. The agreement of the retrieved results and the simulated results verify that this single-sided left-handed metamaterial can exhibit a low loss and broad negative refraction passband, by comparing with the off-plane case and the in-plane case. Furthermore, this single-sided structure metamaterial can ease the fabrication, so it will be a better selection in constructing the LHMs, especially at a high frequency.

ACKNOWLEDGMENT

This work was supported by the National Natural Science Foundation of China under Contract No. 10775055.

[1] V. G. Veselago, Sov. Phys. Usp. **10**, 509 (1968).
[2] D. R. Smith, W. J. Padilla, D. C. Vier, S. C. Nemat-Nasser, and S. Schultz, Phys. Rev. Lett. **84**, 4184 (2000).
[3] J. B. Pendry, A. J. Holden, W. J. Stewart, and I. Youngs, Phys. Rev. Lett. **76**, 4773 (1996).
[4] J. B. Pendry, A. J. Holden, D. J. Robbins, and W. J. Stewart, IEEE Trans. Microwave Theory Tech. **47**, 2075 (1999).
[5] R. A. Shelby, D. R. Smith, and S. Schultz, Science **292**, 77 (2001).
[6] K. Aydin, K. Guven, M. Kafesaki, L. Zhang, C. M. Soukoulis, and E. Ozbay, Opt. Lett. **29**, 2623 (2004).
[7] T. M. Grzegoczyk, C. D. Moss, J. Lu, X. Chen, J. Pacheco, Jr., and J. A. Kong, IEEE Trans. Microwave Theory Tech. **53**, 2956 (2005).
[8] E. Ozbay, K. Guven, and K. Aydin, J. Opt. A, Pure Appl. Opt. **9**, S301 (2007).
[9] V. Shadrivov, D. A. Powell, S. K. Morrison, Y. S. Kivshar, and G. N. Milford, Appl. Phys. Lett. **90**, 201919 (2007).
[10] W. Zhu, X. Zhao, and N. Ji, Appl. Phys. Lett. **90**, 011911 (2007).
[11] N. Katsarakis, M. Kafesaki, I. Tsiapa, E. N. Economou, and C. M. Soukoulis, Photonics Nanostruct. Fundam. Appl. **5**, 149 (2007).
[12] M. Bayindir, K. Aydin, E. Ozbay, P. Markoš, and C. M. Soukoulis, Appl. Phys. Lett. **81**, 120 (2002).
[13] E. Ozbay, K. Aydin, E. Cubukcu, and M. Bayindir, IEEE Trans. Antennas Propag. **51**, 2592 (2003).
[14] T. Koschny, M. Kafesaki, E. N. Economou, and C. M. Soukoulis, Phys. Rev. Lett. **93**, 107402 (2004).
[15] M. Kafesaki, Th. Koschny, R. S. Penciu, T. F. Gundogdu, E. N. Economou, and C. M. Soukoulis, J. Opt. A, Pure Appl. Opt. **7**, S12 (2005).
[16] S. O. Brien and J. B. Pendry, J. Phys.: Condens. Matter **14**, 6383 (2002).
[17] Y. Liu, N. Fang, D. Wu, C. Sun, and X. Zhang, Appl. Phys. A: Mater. Sci. Process. **87**, 171 (2007).
[18] H. Liu, D. A. Genov, D. M. Wu, Y. M. Liu, J. M. Steele, C. Sun, S. N. Zhu, and X. Zhang, Phys. Rev. Lett. **97**, 243902 (2006).
[19] X. Chen, T. M. Grzegorczyk, B.-I. Wu, J. Pacheco, Jr., and J. A. Kong, Phys. Rev. E **70**, 016608 (2004).
[20] D. R. Smith, D. C. Vier, Th. Koschny, and C. M. Soukoulis, Phys. Rev. E **71**, 036617 (2005).
[21] P. Markoš and C. M. Soukoulis, Phys. Rev. E **65**, 036622 (2002).
[22] F. Zhang, G. Houzet, E. Lheurette, D. Lippens, M. Chaubet, and X. Zhao, J. Appl. Phys. **103**, 084312 (2008).